`Noah B Lemke, PhD
4921 Crawford St 3
Houston, Texas, USA 77004
E-mail: noahlemke22@gmail.com
Phone: US +1 630 347 3302

RESEARCH ARTICLE: Temporal Trends: Phase-shifted time-series analysis reveals highly correlated reproductive behaviors in the black soldier fly, *Hermetia illucens* (Diptera: Stratiomyidae)

AUTHORS
Noah B Lemke 1, Chujun Li 2,3, Jeroen De Smet 4, Jeffery K Tomberlin 1

AFFILIATIONS
1 - Department of Entomology, 370 Olsen Blvd Suite 412, Texas A&M University, College Station, Texas, USA 77843
2 - Sun Yat-Sen University, Guangzhou, Guangdong, China
3 - Guangzhou Unique Biotechnology, Room 1717, 101 Science Avenue, Huanpu District, Guangzhou, Guangdong, China
4 – Research Group for Insect Production and Processing, Department of Microbial and Molecular Systems, KU Leuven, Campus Geel, Kleinhoefstraat 4, 2440 Geel, Belgium

* To whom correspondences should be addressed: noahlemke22@gmail.com

ENGLISH ABSTRACT (213 words)

For those researching reproduction of the black soldier fly (BSF), finding meaningful correlations between mating and downstream reproductive fitness metrics, owing to complex reproductive behavior and physiology, has been challenging. On the one hand, mating is not necessarily deterministic of fertile eggs being produced, since females might lay unfertile eggs both before and after mating. But conversely, the process is not 'random' either, since fertility is predicated on the exchange of gametes during mating. To investigate the relationship between mating and other reproductive metrics, a cross-correlation analysis between lagged time series was conducted on data previously collected during a semi-outdoor greenhouse experiment. This process compared the average percent correlation between un-lagged mating with oviposition in traps, oviposition outside traps, total weight of eggs deposited, and hatch rate, which were lagged 0 to −6 days. This revealed that average mating was 97.54% correlated with oviposition in traps lagged by −2 days. For oviposition outside of traps, total egg weights, and hatch rate, these were also ~71.63% correlated, 60.29% correlated, and 75.16% correlated with mating respectively, which were optimized when the time series were lagged n = −3 days. These trends likely have a biological basis since flies decrease their reproductive activity as they expend energy and senesce, aligning with temporal patterns consistently observed during BSF rearing.

KEYWORDS

Reproduction, breeding, optimization, fitness, statistics

INTRODUCTION

Insect reproductive behavior is complex (Lemke et al. 2023, Meneguz et al. 2023, Tomberlin et al. 2025) owing not only to the wide diversity in mating systems and reproductive modes across species (Kokko et al. 2014, Normark 2014), but also the plethora of alternative mating tactics, dynamic evolutionary optimums for fitness, phenotypes, and personas expressed by populations or individuals of the same species (Shuker and Simmons 2014). As an emergent phenomenon (Macklem 2008), reproductive behavior is influenced by several echelons of processes occurring either at a lower organization level or earlier during the life of an insect. These include social context hormonal state, physiology and gross anatomy, nutritional legacy, cellular processes, genetics, eco-evolutionary history (Alcock and Thornhill 2014) and much more. On top of this, empiricists must also consider the covariates and intermediate factors that can act on behavioral outcomes, such as the testing environment or artifacts of the experimental design (Tomberlin et al. 2025). As such, this level of complexity can require sophisticated analytical techniques (Smetana et al. 2025), as well as a broad intuition of insect biology.

Take for example the black soldier fly (BSF), *Hermetia illucens* (L.) (Diptera: Stratiomyidae), which is a large lekking fly (Tomberlin and Sheppard 2001) of neotropical origin (Kaya et al. 2021). BSF has been recently domesticated (Rhode et al. 2020) and is now mass-reared throughout the globe for various applications, such as waste management and subsequent conversion of these materials into insect biomass that can serve as alternative feed ingredients for pets and livestock. For this reason, the operation costs of mass-rearing facilities still need to be driven down to make facilities more economic since the goal of a mass-culture program is to

43 produce the maximum number of fertile females in as short of time and inexpensively as possible
44 with minimal labor and space (Boller 1972).

45 Due to protandry, adult males emerge from pupae prior to females (Tomberlin et al. 2002,
46 Generalovic et al. 2025). However mating studies typically control for both age and sex by taking
47 a portion of reared flies and sorting them to create test populations (e.g., 100 males and 100
48 females). In addition, the labor to sort these flies can be extensive and time consuming, and so a
49 narrow range of ages can be expected (e.g., 0-3 days; 1-4 days). This approach can be contrasted
50 with the industrial process, in which one (or several) batch of pupae are placed directly inside a
51 cage, or in an area adjacent to the cage and allowed to emerge (Coudron et al. 2025). If multiple
52 batches of pupae are added to the cage continuously, then this can lead to the breeding cage
53 containing flies of many mixed ages and reproductive statuses (Dickerson et al. 2024, Lemke et
54 al. 2025), since post-reproductive adult flies might live several weeks or more (Harjoko et al.
55 2023), especially when supplemented with sugar-water or honey (Thinn and Kainoh 2022, Klüber
56 et al. 2023, Barrett et al. 2025), and mating has been shown to extend female longevity (Harjoko
57 et al. 2023) potentially through sperm digestion (Manas et al. 2024).

58 Irrespective of the exact method used to stock cages, what follows is that high densities of
59 individuals engage in 'lek' mating which typically plateaus 2-3 days post-emergence. Males are
60 drawn towards UV-light (Zhang et al. 2010), and females temporarily join these aerial swarms to
61 mate (Lemke et al. 2024). After an aerial courting ritual, copulation commences when male and
62 female lock genitalia and remain nearly motionless on the floor or walls of the cage for ~35 minutes
63 (Manas et al. 2025). Near the end of this time, sperm is transferred via the male's aedeagus into
64 the female (Manas et al. 2025), the two separate, and groom themselves (Laudani et al. 2024).

Following this, there is an intermittent period of several days (Tomberlin and Sheppard 2002) where sperm travels through the female's genital tract (Malawey et al. 2019) and is stored in their spermathecae until the moment of oviposition (Manas et al. 2024), whereupon the eggs are fertilized. To induce egg-laying, an attractant is then introduced (which can be a natural substrate, or a synthetic blend pumped through the cage) to entice females to lay their eggs in a trap. Oviposition activity typically then peaks between days 5-6 days post-emergence. To lay their eggs, females normally seek out an area of dry cracks adjacent to a larval rearing substrate (but obviously such a substrate may not actually be present if the attractant is a synthetic blend). Traps are then replaced, and any deposited eggs are harvested by technicians. 2-5 days later, the neonates hatch from their eggs and begin wandering towards food (Giannetti et al. 2022).

One major area complicating analysis is the temporal structure of the data. Mating and oviposition activity peak several days apart (Tomberlin and Sheppard 2002, Dickerson et al. 2024, Meyermans et al. 2025). Moreover, outside of these peaks there is very little activity, leading count data to be highly zero-inflated (Smetana et al. 2025). To capture information about both, observational experiments need to be run for several days (Chiabotto et al. 2024, Dickerson et al. 2024, Lemke et al. 2024), which presents a logistical hurdle because, unless remote videography is used, human observations cannot accurately be made across this whole time period. A trade-off then exists between capturing data across the entire cycle (e.g. during daylight hours for 1 week) or focusing more narrowly on a particular period (e.g., the time-windows for mating or oviposition). Furthermore, the temporal delay between copulation (i.e., mating), oviposition, and eggs hatching has historically made predicting the values of one from the others difficult, leading some reports to say that mating is only loosely related to the latter (Dickerson et al. 2024).

Hence, the objective of this study is to provide an additional statistical tool for those wishing to monitor the success of their BSF colonies with regards to fertile egg production. This study examined whether the correlation between BSF mating and other reproductive metrics could be improved through phase shifting the time series data for the latter metrics. While the procedures for time series analyses are formalized and widely used in the social sciences, biology, and economics (Shumway and Stoffer 2017a), such analyses are quite new when it comes to interpreting black soldier fly mating data (Lemke et al. 2024). We hypothesized that by adjusting the lag between time series, that mating could be a useful predictor of downstream fitness metrics such as oviposition, total egg weight, and hatch rate.

METHODS

Data Acquisition — Data for this analysis was originally collected as part of a semi-outdoor greenhouse study conducted at the F.L.I.E.S. Facility at Texas A & M University throughout 2022 (Lemke et al. 2025). The original experiment investigated the interaction between BSF cohort age and oviposition attractant provisioning on fitness but did conduct a time-series analysis. 4 trials took place from (a) March 07-13, (b) April 25-May 01, (c) October 06-12, and (d) December 10-16, each lasting 7 days. During these observation periods, count data for mating and oviposition were recorded hourly from sunrise to sunset, while eggs traps were collected daily from cages at noon and the total weight of collected eggs measured gravimetrically. After a 5-day incubation period, hatch rate of the eggs for each collection was also assessed. A full description of the experimental design can be found in Lemke et al., 2025; and similar procedures have been used in other studies (Dickerson et al. 2024, Laursen et al. 2024, Lemke et al. 2024). During each trial, 4

experimental treatments (see below) were tested on the production of a 0.93 m3 breeding cage, supplied with 100 male and 100 female BSF. Each of these 4 treatments was replicated 3 times, for a total of 12 experimental units, yielding 336 cage-days of observations (4 treatments x 3 replicates x 2 blocks x 2 trials x 7 days).

Data Structure & Cleaning — The levels of the original experiment's treatment categories followed a 2 × 2 factorial design, with attractant provisioning having four total combinations of levels (i.e., (a) whether the attractant provided initially or (b) delayed until 1-days post peak mating; and (c) whether the attractant contained substrate or (d) was an empty control). Additionally, age group also had an additional two blocks (two trials each, of which all flies were either "mixed" or "same" age). For the age groups, "young" flies were 1-4-day-old prior to their introduction into mating cages, whereas the "mixed" cohort could have ages between 1-16-days.

However, because industrial producers of BSF do not delay the age of their flies prior to release, for this analysis, we only considered data for the "young" treatment in which this artifact was absent. Likewise, providing attractant boxes lacking attractant is also not representative of industrial rearing conditions and was included in the original experiment as a negative control, but was not taken into consideration for this analysis. Moreover, recent evidence has shown that virgin females have no inherent preference towards a group of volatile organic compounds (VOCs) that later caused attraction or avoidance behaviors in mated females (Klüber et al. 2024). And so, in addition to "mixed" age flies, replicates for which there was never an attractant provided (labeled as "IC" and "DC" respectively for Initial and Delayed Controls) were redacted from the data set. This yielded 168 rows of data (2 trials × 12 cages × 7 days) (i.e., half of the original 336 cage-days) that could further be grouped by cage position (i.e., #1-12). The reduced data frame

(containing only data from "young" flies that were provided attractant initially = "IO" or delayed "DO") was then reformatted using the PivotTable function in MS Excel for Mac Version 16.97 (25051114), to make calculating the averages much easier.

Time Series Analysis — To examine temporal patterns, the data were plotted using MSExcel inbuilt plotting function. By averaging values by day (of observations taken hourly from sunrise to sunset) autoregression (as used by Lemke et al. 2024) was not necessary for this analysis because there were no gaps in the data that needed to be filled. Visually inspecting the plots revealed that phase shifting the data might lead to stronger cross-correlations, since mating and oviposition follow a similar temporal pattern, albeit with oviposition lagging by two days.

Percent Correlation Coefficient Matrix — To make cross-correlations, a Pearson correlation matrix was constructed which included all pairwise combinations for mating and oviposition across treatments. For example, the mating-oviposition (in traps) matrix considered the mean average of IO-mating, as correlated to the mean average of DO-mating, IO-oviposition, and DO-oviposition. For the resulting matrix, only the lower triangle of correlation coefficients (i.e., cells underneath the identity diagonal) were considered since the matrix was symmetrical. Values were then squared (r-squared), which is also considered a measure of effect size (Rights and Sterba 2020), and multiplied by 100 to yield the percent correlation coefficient (PCC). From this, the average Pearson PCC of the matrix was calculated (i.e., by summing all values and dividing by the number of values within the lower triangle), as well as the standard deviation and standard error (of n = 6 values under the diagonal). For this step, Pearson's correlation was chosen to investigate when a linear increase in mating corresponded to a linear increase in oviposition, or

vice versa. However, using Spearman's rank correlation would allow a looser interpretation in which an increase in mating corresponded to *any* increase in oviposition, not necessarily a linear one (and was used in the Clustered Heat Map analysis below).

Phase Shifted PCC — Next, a series of PCC matrices were calculated to determine what among of phase shifting optimized PCC. This was done for each pair of reproductive metrics (mating with mating = autocorrelation, mating with oviposition in traps, mating with oviposition in cages, mating with total egg weight, and mating with hatch rate). Data were phase shifted n = 0, −1, −2, −3, −4, −5, and −6 days, yielding $y_t, y_{t-1}, y_{t-2}, \ldots y_{t-6}$. To phase shift the data, the first n-days of the data were deleted and the remainder shifted forward, creating an empty tail that was filled with 0-values in order to preserve the length of the time series. Mating was always kept 'un'-shifted, primarily because it occurs first in the mating sequence (and so is more biologically relevant), but also to reduce the total number of symmetrical combinations (e.g., when both mating and oviposition were phase shifted equivalently). The average PCC across this continuum of phase shifting was then plotted in MSExcel and examined visually to determine candidates for optimization by finding local maxima/minima.

Clustered Heat Map — Finally, a clustered heat map was generated for all metrics combined. This was constructed by first calculating the pairwise Spearman rank correlation between reproductive metrics that were both unmodified as well as phase shifted. The number of days that each metric was phase shifted was determined by taking the number of days that optimized the average PCC in the above analysis and also using their neighboring values of ± 1 day (i.e., if an optimum was found for oviposition with a phase shift of n = −2, then this along with n = −1 and n = −3 were

considered). The correlation matrix was calculated using the corr() function in RStudio (Wei and Simko 2024), using Spearman's rank coefficient (since the functions above were not strictly monotonic). These values were then plotted as a clustered heatmap using the corrplot() function in RStudio.

RESULTS

Visual Analysis — As a first step, data for mating x day, oviposition x day, total egg weight x day, and hatch rate x day was visualized by plotting in MS Excel. Raw values with ± SD can be found in Table S1 and were plotted in MS Excel (Figures 1, 2). Doing this revealed average mating peaked on day 1 (of the cycle), whereas average oviposition peaked on day 4. The trend for each was to generally decrease following this peak, however mating was not strictly monotonic, in that there was a second small peak between days 3-4. Cumulative average total egg weight and hatch rate both plateaued by day 5, with daily values generally decreased after reaching a peak on day 3. Qualitatively, it then appeared that mating would have the strongest correlation to oviposition when the latter was shifted forward n = −2 days. However, because of the plateau, total egg weight and hatch rate might be more strongly correlated with mating when phase shifted greater than −1 days.

Cross Correlation of Time Series Data — The initial analysis considering Mating x Oviposition for each treatment was optimized when oviposition was lagged by −2 days, with individual values within the matrix ranging from 97.56 - 98.66 PCC (Table S2), indicating that PCC could be optimized by lagging data. Hence, for each reproductive metric, the average Pearson correlation

coefficient was calculated between mating, and that second metric phase shifted by n = 0, −1, −2, −3, −4, −5, and −6 days. These were then plotted to visually inspect where (local) optima lie. Mating autocorrelation (Figure 3) was minimized for a 1-day lag (34.48%), and highest for a 3-day lag (96.10%). The comparison between mating and oviposition (in traps), average PCC was maximized with a phase shift of n = −2 days. Doing this increased the PCC from 31.19% to 97.54%, a 3.12-fold difference (Figure 4). For the comparison between mating and oviposition (in cage material) (Figure 5), average PCC was maximized with a −3-, −4-, or −5-day time lag (~72%) and minimized with a 0-day time lag (19.71%). For the comparison between mating and total egg weight (Figure 6), a local maximum was found with a −3-day lag (60.29%) up from 29.22% with no lag, representing a 2.06-fold increase. Interestingly though, the highest value was for total egg weight with −6-day time lag, though this is suspected to be a statistical artifact (see Discussion below), and for this reason the local optima at n = −3 days is preferred. Lastly, the comparison between mating and hatch rate (Figure 7) also had a maximized average PCC with a −3-day lag (75.16%) up from 40.48%, representing a 1.85-fold increase.

Clustered Heat Map — A clustered heat map was constructed to reveal grouped relationships between mating and downstream reproductive metrics that were either not phase shifted or those that were phase shifted a number of days (±1), equal to the optima found in the previous step. Within the clustered heat map, mating was found in a cluster together with oviposition (in traps) phase shifted 2 and 3 days. This cluster was most closely related to a larger cluster containing total egg weight phase shifted −2 and −3 days well as hatch rate phase shifted −2 days and −3 days. Interestingly, the most distant cluster to mating contained the original unmodified oviposition in

traps, total egg weight, and hatch rate metrics, as well as oviposition in cages phase shifted −3 days.

DISCUSSION

The objective of this study was to examine whether correlations between time series data of reproductive metrics recorded during a BSF breeding study could be improved by comparing time series that were phase shifted/lagged. Since there is an obvious temporal component to mating behaviors, this study greatly improves upon that of Lemke et al. 2025 who did not consider time series analyses as part of the original study, focusing instead on statistical differences between treatment effects. Indeed, the results of this analysis show that lagging the data forward in time increased the Pearson percent correlation coefficient (PCC), i.e., effect size, between mating and other downstream reproductive metrics substantially. By doing this, mating was 97.56 to 98.66% correlated with oviposition in traps when the latter was lagged −2 days. Likewise, for oviposition outside of traps, total egg weights, and hatch rate, these were ~71.63% correlated, 60.29% correlated, and 75.16% correlated with mating respectively, which were optimized when the time series were lagged n = −3 days. A clustered heat map confirmed this relationship, showing mating was most closely related (i.e., had the strongest correlation) with a cluster of metrics that included oviposition, total egg weight, and hatch rate, that were each phase shifted by these optima. In addition, the clustered heat map showed that mating was also least correlated with these same fitness metrics if they were unmodified. Thus, this experiment highlights the importance for BSF producers to considering correlations between reproductive metrics measured at different time points in production, as well as understanding whether these correlations are rooted in biology.

At first glance, the link between mating and these lags generally corresponded biologically to temporal patterns within the data. The initial visual inspection of the reproductive metrics (plotted by day) revealed that mating peaked on Day 1 (Figure 1). The trend for the mating time series was then generally decreased but had a small 'hump' on days 3-4 (Figure 1). This suggested that individuals can engage in multiple matings, as did the fact that mating autocorrelation was maximized on these same days (Figure 3). Indeed, the multiple mating in BSF for both males and females has now been verified by many recent experiments (Hoffmann et al. 2021, Chiabotto et al. 2024, Muraro et al. 2024). Similarly, oviposition in traps peaked on day 3 and then decreased monotonically (Figure 1), meaning the distance between peak mating and peak oviposition (occurring on Days 1 and 3, respectively) was $n = -2$ days. This was equivalent to the optimized time lag (Table S1, Figure 4).

Interestingly, the peak for total egg weight occurred prior to the peak for oviposition counts in traps (Figures 1, 2), indicating that perhaps larger egg clutches are laid by females earlier in the cycle, and smaller ones later in the cycle. A prior experiment reports multiple oviposition events, but that subsequent clutches were smaller and infertile (Nakamura et al. 2016). Alternatively, it could also mean that later in the cycle there are instances where females extend their ovipositors but do not lay eggs (reflecting an inaccuracy in the original data set). Lastly, hatch rate peaked on day 3 (i.e., eggs laid on day 3 had the highest hatch rate after their 5-day incubation period). The hatch rate then decreased monotonically, suggesting that the process of sperm storage within the female takes ~2 days (since before day 3 the hatch of any eggs collected is relatively low), aligning with a recent report (Manas et al. 2024). Alternatively, because the data were gathered in an semi-outdoor environment, it could also be that this peak in fertility corresponded to days with more

269 optimal environmental conditions, such as higher humidity that might reduce desiccation, or
270 ambient temperatures falling within thermal tolerances (Chia et al. 2018, Addeo et al. 2022).

271 Another interesting pattern in the data is that the PCC between mating and oviposition
272 (inside of cages) peaked earlier than did the PCC between mating and oviposition (outside of
273 cages), which seem to correspond to a 1-day earlier peak in oviposition in traps versus cages
274 (Figure 1). Since the data used here include only 1-4-day-olds, the uptick in oviposition outside of
275 cages can't easily be explained by delayed mating, as was the case for prior experiments which
276 did this to created aged test-populations (Dickerson et al. 2024, Lemke et al. 2025). Instead, the
277 pattern might indicate that the flies become less discriminating as they age. There could also be an
278 environmental effect, whereby the temperature happened to increase on those days (for both trials),
279 forcing the flies away from ovipositing in the trap, which absorbed/reflected a lot of heat (Lemke
280 et al. 2025). Another explanation could also be a snowball-effect whereby day 4-5 of the
281 experiment, some flies had haphazardly laid eggs in the cage material early on, and then the
282 volatiles from those eggs (Klüber et al. 2023) attracted additional flies to lay outside of the trap.

283 The temporal trends reported here generally align with what has been observed in previous
284 BSF breeding experiments (Tomberlin and Sheppard 2002, Zhang et al. 2010). For example, early
285 experiments on BSF showed that mating peaked on days 1-2, with oviposition peaking several
286 days later (Tomberlin and Sheppard 2002, Park et al. 2010). This has been a consistent trend in
287 mating experiments to this date (Jones and Tomberlin 2021, Dickerson et al. 2024, Lemke et al.
288 2024, Meyermans et al. 2025). In addition, more recent studies have demonstrated multiple mating
289 (Hoffmann et al. 2021, Chiabotto et al. 2024, Muraro et al. 2024), multiple oviposition (Muraro et
290 al. 2024), and physiological processes occurring during these 'lulls' in activity (Manas et al. 2024),
291 as well as the potential for a neurophysiological switch during this time for females to become

receptive to volatiles (Klüber et al. 2024). As such, it is reassuring to know that these patterns continue to hold true after two decades of BSF rearing, both throughout the globe, as well as in indoor and semi-outdoor rearing conditions.

However, because the original trend for mating in this experiment was to generally decrease after day 1, the Pearson PCC between mating and any other reproductive metric appears to have been optimized when the phase shift applied also transformed the time series to become a monotonic decreasing function. Of course, this is reflective of the fact that the original experiment only used a single batch of flies per cage, and it is expected that this trend will not hold true once new flies are added to cages through continuous rearing (see below for suggested analysis to perform in this case). For the batch-reared data analyzed here, although mating was not strictly monotonic, in general its trend was to decrease. In effect, the high correlations may be a statistical artifact (i.e., a spurious correlation) resulting from qualitatively similar trends between un-lagged mating (i.e., decreasing) with the lagged oviposition or another lagged metric (i.e., transformed to become decreasing). Such was also seen in the temporal autocorrelation function for mating, which was lowest between days 0 and 1. Lagging the data n = -1 days effectively removed the peak on day 1, and made the new mating peak occur between days 3-5 (shifted to days 2-4). Hence, autocorrelation was highest on days 3-5, because lagging the function by this amount effectively transformed it into a strictly decreasing (i.e., monotonic) function. Likewise, the PCC between mating (unadjusted) and total egg weight was highest when egg weight was lagged by −6 days (creating a strictly decreasing function to qualitatively match mating). Still, these trends have a biological basis that resonates with long held understanding of temporal patterns in BSF reproduction, in which reproductive activity decreases with time as flies exhaust their energy stores, and senesce (Harjoko et al. 2023, Dickerson et al. 2024). Additionally, the cumulative

distribution for total egg weight (i.e., by adding each day's value to the previous sum) plateaus around n = −6 days, corresponding with the global maximum PCC.

Of course, correlation does not imply causation, but to some extent we can infer directionality since mating generally occurs prior to oviposition, oviposition before any eggs are collected, and total egg weight necessarily occurring before any are hatched. In addition, all these quantities intuitively must co-vary with one another, given that they are predicated on optimized abiotic conditions (e.g., light, temperature, humidity).

Limitations and how to adapt this study for Industry — This analysis is limited largely because it uses a dataset collected from two disjunct rearing cycles only lasting 7 days each. For industrial programs that might need to produce high volumes of eggs/neonates, this analysis could be applied but would need to be modified in one of the following ways:

First, for those practicing batch rearing (Coudron et al. 2025, Lemke et al. 2025), mating might instead peak on day 2 or 3 of a breeding cycle rather than day 1 which would make sense due to differences in the emergence time between males and females (i.e., protandry) or their initial period of inactivity. In this case, since monitored mating activity would increase suddenly and then decrease, the mating time series would no longer be monotonic, and might be qualitatively similar to some of the other reproductive metrics. Similarly, the time series might be non-monotonic if BSF experience several activity peaks as a result of multiple mating. In either case, a Spearman's Rank correlation could be calculated instead of Pearson's to loosen some of the assumptions and examine increases in non-monotonic functions, which is what was done to construct the clustered heat map presented here (Figure 8, Table S2).

If instead, a producer operates their breeding cages continuously (Dickerson et al. 2024, Coudron et al. 2025, Lemke et al. 2025), then it might be better to calculate a rolling window (i.e., a fixed time frame of e.g. 7 days, calculated each day) from which long term temporal patterns could be ascertained (such as, whether mating on certain days is correlated with oviposition on others, or whether there are weekly and seasonal trends across operations). Such patterns could be also modeled arithmetically through an ARIMA model (Shumway and Stoffer 2017b), which are traditionally used in stock price and commodities forecasting. Application of this technique will be complex however if there is a non-stationary trend or autocorrelation between rearing cycles (i.e., decreases over time due to genetic deterioration, or increases corresponding with sudden increases in population density).

The extent to which these are practical to implement for BSF breeding will of course depend on the elegance of behavioral assays and the information gleaned from them (Tomberlin et al. 2025). Standard metrics like egg weight and hatch rate, which are simple enough to measure gravi-, or volu-, metrically, can of course be formatted as Time Series data as has been done here. In addition, there are also many remote detection methods proposed for use in insect agriculture (Manoukis and Collier 2019, Nawoya et al. 2024), and some have started to be realized. These include FlyCount (James et al. 2024), a program that monitors population density of adults passing through a narrow opening prior to entering the breeding cage, as well as HistoNet (Sharma et al. 2020) to automatically assign size-classes to BSF. Counting the number of flies in a cage, recording their sizes, and monitoring fertile egg production in relation to these factors longitudinally (Dickerson et al. 2024) will be one step, but an important one, towards understanding the system and increasing its predictability in a complex system.

ACKNOWLEDGEMENTS

We would like to thank our anonymous reviewers, as well as the group of researchers who helped collect the original data set: Amy J. Dickerson, D. A. Salazar, J. Emmanuel Mendoza, Lisa N. Rollinson, Erin Harris, Sienna McPeek, Rachel MacNeal, and Drs. Chelsea Miranda, and Casey Flint.

This material is based upon work supported by the National Science Foundation Graduate Research Fellowship under Grant No. 1746932. Any opinion, findings, and conclusions or recommendations expressed in this material are those of the authors and do not necessarily reflect the views of the National Science Foundation. This research was also partially supported by funds from the US State Department and the Belgium-Luxembourg Fulbright Commission under the 2026 US-Belgium Fulbright Scholar Program. The content of this report is explicitly that of the authors and does not reflect the views of the Fulbright Program, nor the governments of the United States, Belgium, or Luxembourg.

CONFLICT OF INTEREST

The data analyzed in this study were derived from material purchased from EVO Conversion Systems LLC, a company with which JK Tomberlin has historically had a significant financial interest. This conflict of interest is managed by a plan submitted to and approved by Texas A&M University and Texas A&M AgriLife.

REFERENCES

Addeo NF, Li C, Rusch TW, et al. 2022. Impact of age, size, and sex on adult black soldier fly *Hermetia illucens* L. (Diptera: Stratiomyidae) thermal preference. Journal of Insects as Food and Feed. 8(2):129–139. https://doi.org/10.3920/JIFF2021.0076

Alcock J, Thornhill R. 2014. The evolution of insect mating systems. In: Shuker DM, Simmons LW, editors. Evolution of Insect Mating Systems. Illustrated. United Kingdom: Oxford University Press. p. 78–91.

Barrett M, Patel N, McCarry B, et al. 2025. Dietary preferences and impacts of feeding on behavior, longevity, and reproduction in adult black soldier flies (Diptera: Stratiomyidae; *Hermetia illucens*). https://doi.org/10.31219/osf.io/p74xq_v1

Boller E. 1972. Behavioral aspects of mass-rearing of insects. Entomophaga. 17(1):9–25. https://doi.org/10.1007/BF02371070

Chia SY, Tanga CM, Khamis FM, et al. 2018. Threshold temperatures and thermal requirements of black soldier fly *Hermetia illucens*: Implications for mass production. PLOS ONE. 13(11):1–26.

Chiabotto C, Grosso F, Doretto A, et al. 2024. Observation of mating behavior using marked flies of black soldier fly (*Hermetia illucens*) under sunlight condition. Journal of Insects as Food and Feed. 10(12):2017–2029. https://doi.org/10.1163/23524588-20230165

Coudron CL, Adamaki-Sotiraki C, Yakti W, et al. 2025. Bugbook: Basic information and good practices on how to maintain stock populations for *Tenebrio molitor* and *Hermetia illucens* for research. https://doi.org/10.1163/23524588-bja10240

Dickerson AJ, Lemke NB, Li C, et al. 2024. Impact of age on the reproductive output of *Hermetia illucens* (Diptera: Stratiomyidae). Crippen T, editor. Journal of Economic Entomology.:toae107. https://doi.org/10.1093/jee/toae107

Generalovic TN, Zhou W, Zhao LC, et al. 2025. Repeatable phenotypic but not genetic response to selection on body size in the black soldier fly. :2025.02.25.640052. https://doi.org/10.1101/2025.02.25.640052

Giannetti D, Schifani E, Reggiani R, et al. 2022. Do it by yourself: Larval locomotion in the black soldier fly *Hermetia illucens*, with a novel “self-harvesting” method to separate prepupae. Insects. 13(2):127. https://doi.org/10.3390/insects13020127

Harjoko DN, Hua QQH, Toh EMC, et al. 2023. A window into fly sex: mating increases female but reduces male longevity in black soldier flies. Animal Behaviour. 200:25–36. https://doi.org/10.1016/j.anbehav.2023.03.007

Hoffmann L, Hull KL, Bierman A, et al. 2021. Patterns of genetic diversity and mating systems in a mass-reared black soldier fly colony. Insects. 12(6):480. https://doi.org/10.3390/insects12060480

James A, Seth A, Marcireau A, et al. 2024. FlyCount: High-speed counting of black soldier flies using neuromorphic sensors. IEEE Sensors Journal.:1–1. https://doi.org/10.1109/JSEN.2024.3504289

Jones BM, Tomberlin JK. 2021. Effects of adult body size on mating success of the black soldier fly, *Hermetia illucens* (L.) (Diptera: Stratiomyidae). Journal of Insects as Food and Feed. 7(1):5–20. https://doi.org/10.3920/JIFF2020.0001

Kaya C, Generalovic TN, Ståhls G, et al. 2021. Global population genetic structure and demographic trajectories of the black soldier fly, *Hermetia illucens*. BMC Biol. 19(1):94. https://doi.org/10.1186/s12915-021-01029-w

Klüber P, Arous E, Jerschow J, et al. 2024. Fatty acids derived from oviposition systems guide female black soldier flies (*Hermetia illucens*) toward egg deposition sites. Insect Science. 31(4):1231–1248. https://doi.org/10.1111/1744-7917.13287

Klüber P, Arous E, Zorn H, et al. 2023. Protein- and carbohydrate-rich supplements in feeding adult black soldier flies (*Hermetia illucens*) affect life history traits and egg productivity. Life. 13(2):355. https://doi.org/10.3390/life13020355

Kokko H, Klug H, Jennions MG. 2014. Mating systems. In: Shuker DM, Simmons LW, editors. Evoltuion of Insect Mating Systems. Illustrated. United Kingdom: Oxford University Press. p. 78–91.

Laudani F, Campolo O, Latella I, et al. 2024. Does *Hermetia illucens* recognize sibling mates to avoid inbreeding depression? entomologia. 44(5):1225–1232. https://doi.org/10.1127/entomologia/2024/2746

Laursen SF, Flint CA, Bahrndorff S, et al. 2024. Reproductive output and other adult life-history traits of black soldier flies grown on different organic waste and by-products. Waste Management. 181:136–144. https://doi.org/10.1016/j.wasman.2024.04.010

Lemke NB, Dickerson AJ, Tomberlin JK. 2023. No neonates without adults. BioEssays. 45(1):2200162. https://doi.org/10.1002/bies.202200162

Lemke NB, Li C, Dickerson AJ, et al. 2025. Heterogeny in cages: Age-structure and attractant availability impacts fertile egg production in the black soldier fly, *Hermetia illucens*. Journal of Insects as Food and Feed. Online. https://doi.org/10.1163/23524588-bja10275

Lemke NB, Rollison LN, Tomberlin JK. 2024. Sex-specific perching: Monitoring of artificial plants reveals dynamic female-biased perching behavior in the black soldier fly, *Hermetia illucens* (Diptera: Stratiomyidae). Insects. 15(10):770. https://doi.org/10.3390/insects15100770

Macklem PT. 2008. Emergent phenomena and the secrets of life. Journal of Applied Physiology. 104(6):1844–1846. https://doi.org/10.1152/japplphysiol.00942.2007

Malawey AS, Mercati D, Love CC, et al. 2019. Adult reproductive tract morphology and spermatogenesis in the black soldier fly (Diptera: Stratiomyidae). Annals of the Entomological Society of America. 112(6):576–586. https://doi.org/10.1093/aesa/saz045

Manas F, Labrousse C, Bressac C. 2025. Plastic responses in sperm expenditure to sperm competition risk in black soldier fly (*Hermetia illucens*, Diptera) males. Journal of Insect Physiology. 161:104751. https://doi.org/10.1016/j.jinsphys.2025.104751

Manas F, Piterois H, Labrousse C, et al. 2024. Gone but not forgotten: dynamics of sperm storage and potential ejaculate digestion in the black soldier fly Hermetia illucens. Royal Society Open Science. 11(10):241205. https://doi.org/10.1098/rsos.241205

Manoukis NC, Collier TC. 2019. Computer vision to enhance behavioral research on insects. Annals of the Entomological Society of America. 112(3):227–235. https://doi.org/10.1093/aesa/say062

Meneguz M, Miranda CD, Cammack JA, et al. 2023. Adult behaviour as the next frontier for optimising industrial production of the black soldier fly *Hermetia illucens* (L.) (Diptera: Stratiomyidae). Journal of Insects as Food and Feed. 9(4):399–414. https://doi.org/10.3920/JIFF2022.0055

Meyermans R, Broeckx L, Mondelaers J, et al. 2025. Exploring the potential of crossbreeding to enhance black soldier fly (Hermetia illucens) production. https://doi.org/10.1163/23524588-00001391

Muraro T, Lalanne L, Pelozuelo L, et al. 2024. Mating and oviposition of a breeding strain of black soldier fly Hermetia illucens (Diptera: Stratiomyidae): polygynandry and multiple egg-laying. Journal of Insects as Food and Feed. 1(aop):1–13. https://doi.org/10.1163/23524588-20220175

Nakamura S, Ichiki RT, Shimoda M, et al. 2016. Small-scale rearing of the black soldier fly, *Hermetia illucens* (Diptera: Stratiomyidae), in the laboratory: Low-cost and year-round rearing. Appl Entomol Zool. 51(1):161–166. https://doi.org/10.1007/s13355-015-0376-1

Nawoya S, Ssemakula F, Akol R, et al. 2024. Computer vision and deep learning in insects for food and feed production: A review. Computers and Electronics in Agriculture. 216:108503. https://doi.org/10.1016/j.compag.2023.108503

Normark BB. 2014. Modes of reproduction. In: Shuker DM, Simmons LW, editors. Evoltuion of Insect Mating Systems. Illustrated. United Kingdom: Oxford University Press. p. 78–91.

Park K, Kim W, Lee S, et al. 2010. Seasonal pupation, adult emergence, and mating of black soldier fly, *Hermetia illucens* (Diptera: Stratiomyidae) in artificial rearing system. :3.

Rhode C, Badenhorst R, Hull KL, et al. 2020. Genetic and phenotypic consequences of early domestication in black soldier flies (*Hermetia illucens*). Animal Genetics. 51(5):752–762. https://doi.org/10.1111/age.12961

Rights JD, Sterba SK. 2020. New recommendations on the use of R-squared differences in multilevel model comparisons. Multivariate Behavioral Research. 55(4):568–599. https://doi.org/10.1080/00273171.2019.1660605

Sharma K, Gold M, Zurbruegg C, et al. 2020. HistoNet: Predicting size histograms of object instances. In: 2020 IEEE Winter Conference on Applications of Computer Vision (WACV). Snowmass Village, CO, USA: IEEE. p. 3626–3634. https://doi.org/10.1109/WACV45572.2020.9093484

Shuker DM, Simmons LW, editors. 2014. The evolution of insect mating systems. University of Oxford: Oxford University Press.

Shumway RH, Stoffer DS. 2017a. Time series analysis and Its applications: With R examples. Cham: Springer International Publishing (Springer Texts in Statistics). https://doi.org/10.1007/978-3-319-52452-8

Shumway RH, Stoffer DS. 2017b. ARIMA models. In: Shumway RH, Stoffer DS, editors. Time Series Analysis and Its Applications: With R Examples. Cham: Springer International Publishing. p. 75–163. https://doi.org/10.1007/978-3-319-52452-8_3

Smetana S, Coudron C, Deruytter D, et al. 2025. BugBook: Data analysis methods in studies of insects for food and feed. https://doi.org/10.1163/23524588-bja10209

[Software] Wei T, Simko V. 2024. R package “corrplot”: Visualization of a correlation matrix. https://github.com/taiyun/corrplot.

Thinn AA, Kainoh Y. 2022. Effect of diet on the longevity and oviposition performance of black soldier flies, Hermetia illucens (Diptera: Stratiomyidae). Japan Agricultural Research Quarterly: JARQ. 56(2):211–217. https://doi.org/10.6090/jarq.56.211

Tomberlin J, Sheppard D. 2002. Factors influencing mating and oviposition of black soldier flies (Diptera: Straiomyidae) in a colony. Journal of Entomological Science. 37(4):345–352. https://doi.org/10.18474/0749-8004-37.4.345

Tomberlin JK, Klammsteiner T, Lemke N, et al. 2025. BugBook: Black soldier fly as a model to assess behaviour of insects mass produced as food and feed. https://doi.org/10.1163/23524588-bja10225

Tomberlin JK, Sheppard DC. 2001. Lekking behavior of the black soldier fly (Diptera: Stratiomyidae). Florida Entomologist. 84(4):729–730.

Tomberlin JK, Sheppard DC, Joyce JA. 2002. Selected life-history traits of black soldier flies (Diptera: Stratiomyidae) reared on three artificial diets. an. 95(3):379–386. https://doi.org/10.1603/0013-8746(2002)095[0379:SLHTOB]2.0.CO;2

Zhang J, Huang L, He J, et al. 2010. An artificial light source influences mating and oviposition of black soldier flies, *Hermetia illucens*. Journal of Insect Science. 10(202):1–7. https://doi.org/10.1673/031.010.20201

FIGURE CAPTIONS AND ALT TEXT

FIGURE 1. Plot of time-series data for average mating and oviposition counts. Oviposition counts include for both inside the traps ("OviTrap") and outside the traps ("OviCage"). The experimental unit consisted of a 0.93 m3 cage supplied initially with 100 Male and 100 Female BSF aged 0-4 days. Observations were made each hour from sunrise to sunset for 7 days. Hourly data from 2 experimental treatments (with n = 3 replicate cages for each treatment) was summed to give a total count for each day. Then the totals for the 6 replicates was averaged to give the average total counts with respect to each day.

FIGURE 1 ALT TEXT: Line plot of time-series data for BSF reproductive behaviors. The red line represents average total mating counts. The yellow line represents average total oviposition counts inside traps. The purple line represents the average total oviposition counts outside traps. Below the line plot is a table giving the exact values of each data point.

FIGURE 2. Plot of time-series data for total egg weight (mg) and hatch rate (%) observed in egg traps. The experimental unit consisted of a 0.93 m3 cage supplied initially with 100 Male and 100 Female BSF aged 0-4 days. Eggs were harvested from cardboard traps harvested each day at noon and then weighed. From this, hatch rate for each day's collected eggs was calculated after a 5-day incubation period. Egg weight data were summed to give total weight collected for each day, then the average taken across 6 replicates (n = 2 treatments with n = 3 cages). Because hatch rate was a percentage, instead the mean hatch rate for each day was calculated, then averaged

across the 6 replicates. Full description of egg collection, weighing, and hatch percentage calculations are given in Lemke et al. (2025).

FIGURE 2 ALT TEXT. Line plot depicting average total egg weight and the average mean percent hatch rate. The green line represents egg weight, whereas the blue line represents percent hatch. Beneath the plot is a table giving exact values for each data point.

FIGURE 3. Temporal autocorrelation of mating. Average Pearson percent correlation coefficient between mating (phase shift = 0 days) and mating (phase shifted n = 0, −1, −2, −3, −4, −5, −6 days). Percent correlation was calculated by squaring the Pearson correlation coefficient and multiplying the value by 100. The average of this was taken by summing all values in the lower triangle of the correlation matrix. Error bars presented are ± Standard Error.

FIGURE 3 ALT TEXT: Line plot depicting the autocorrelation between the average Pearson percent correlation between mating counts and mating counts that are phase shifted between 0 and −6 days. Error bars show ± Standard Error.

FIGURE 4. Average Pearson percent correlation coefficient between mating (phase shift = 0 days) and oviposition (phase shifted n = 0, −1, −2, −3, −4, −5, −6 days). Percent correlation was calculated by squaring the Pearson correlation coefficient and multiplying the value by 100. The average of this was taken by summing all values in the lower triangle of the correlation matrix. Error bars presented are ± Standard Error.

FIGURE 4 ALT TEXT: Line plot depicting the autocorrelation between the average Pearson percent correlation between mating counts and oviposition counts in traps that are phase shifted between 0 and −6 days. Error bars show ± Standard Error.

FIGURE 5. Average Pearson percent correlation coefficient between mating (phase shift = 0 days) and oviposition outside of traps (phase shifted n = 0, −1, −2, −3, −4, −5, −6 days). Percent correlation was calculated by squaring the Pearson correlation coefficient and multiplying the value by 100. The average of this was taken by summing all values in the lower triangle of the correlation matrix. Error bars presented are ± Standard Error.

FIGURE 5 ALT TEXT: Line plot depicting the autocorrelation between the average Pearson percent correlation between mating counts and oviposition counts outside traps that are phase shifted between 0 and −6 days. Error bars show ± Standard Error.

FIGURE 6. Average Pearson percent correlation coefficient between mating (phase shift = 0 days) and total egg weight (phase shifted n = 0, −1, −2, −3, −4, −5, −6 days). Percent correlation was calculated by squaring the Pearson correlation coefficient and multiplying the value by 100. The average of this was taken by summing all values in the lower triangle of the correlation matrix. Error bars presented are ± Standard Error.

FIGURE 6 ALT TEXT: Line plot depicting the autocorrelation between the average Pearson percent correlation between mating counts and total egg weights that are phase shifted between 0 and −6 days. Error bars show ± Standard Error.

FIGURE 7. Average Pearson percent correlation coefficient between mating (phase shift = 0 days) and mean hatch rate (phase shifted n = 0, −1, −2, −3, −4, −5, −6 days). Percent correlation was calculated by squaring the Pearson correlation coefficient and multiplying the value by 100. The average of this was taken by summing all values in the lower triangle of the correlation matrix. Error bars presented are ± Standard Error.

FIGURE 7 ALT TEXT: Line plot depicting the autocorrelation between the average Pearson percent correlation between mating counts and mean hatch rates that are phase shifted between 0 and −6 days. Error bars show ± Standard Error.

FIGURE 8. Clustered Heat Map of Time Series Data. The numbers appended to the data labels indicate how many days forward the time series was lagged. “Mating” = Mating. “OviTrap” = Oviposition in traps. “OviCage” = Oviposition in Cages. “EggWeight” = Total Egg Weight. “Hatch” = Hatch rate. Correlation matrix was calculated using Spearman’s rank coefficient. Color formatting is applied with the conditional rule as follows: −1 = 0th percentile (Orange), 0 = 50th percentile (White), +1 = 100th percentile (Blue).

FIGURE 8 ALT TEXT: Clustered heat map indicating that the Spearman’s Rank correlation between mating and the other reproductive metrics is highest when those other metrics are phase shifted −2 days for oviposition in traps and outside of traps, between −2 and −4 days for egg weight, and −3 days for hatch rate.

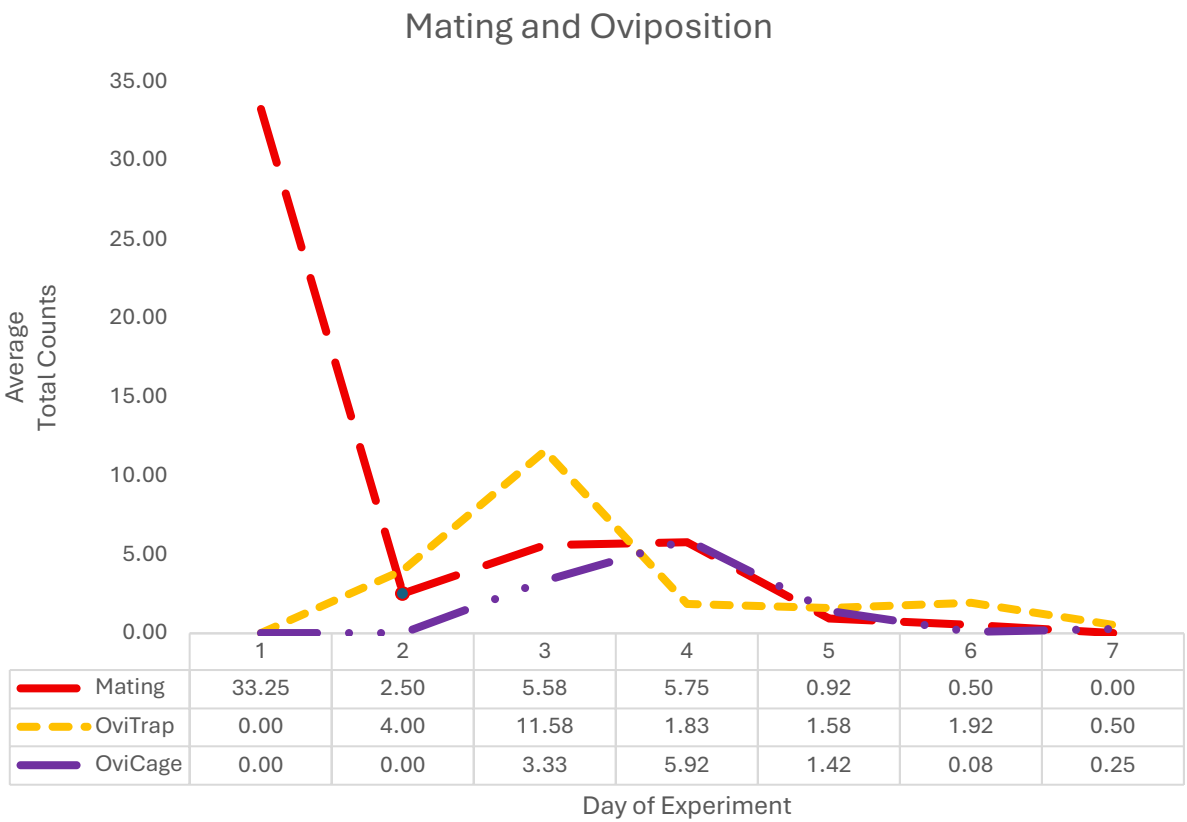

	1	2	3	4	5	6	7
Mating	33.25	2.50	5.58	5.75	0.92	0.50	0.00
OviTrap	0.00	4.00	11.58	1.83	1.58	1.92	0.50
OviCage	0.00	0.00	3.33	5.92	1.42	0.08	0.25

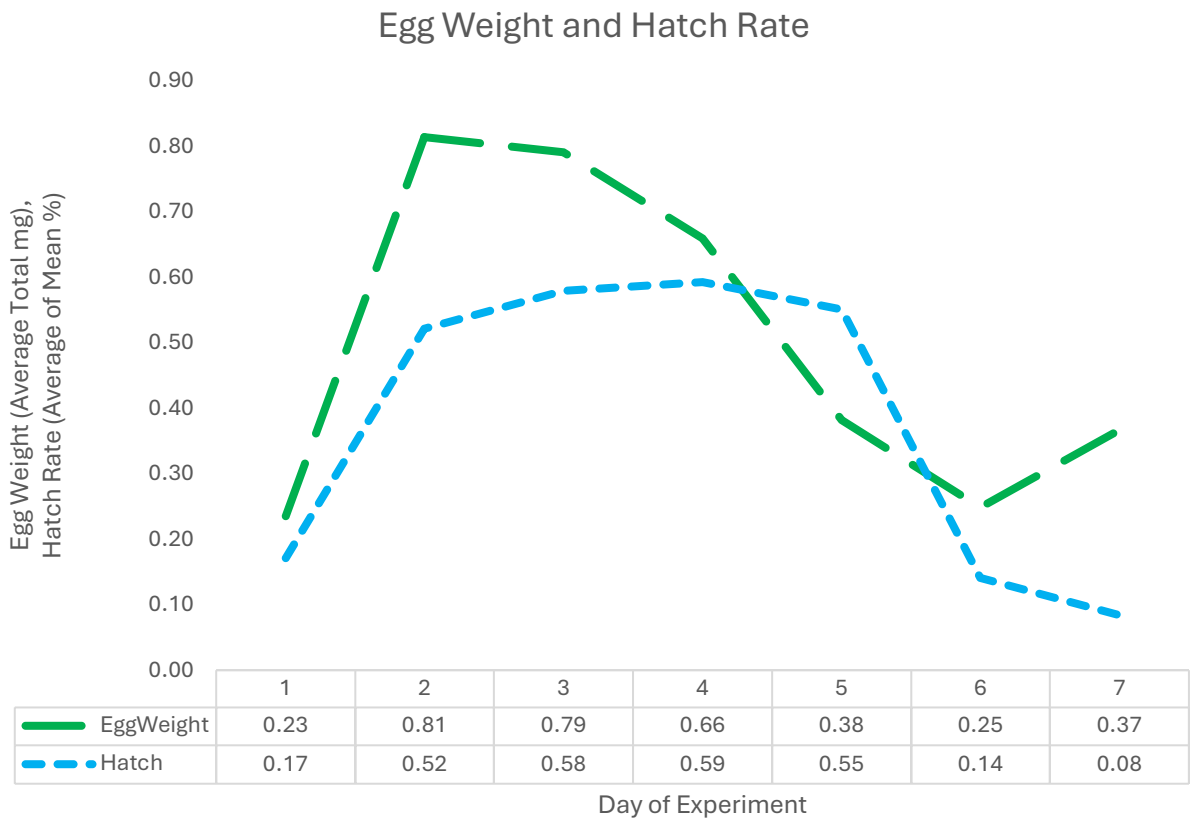

	1	2	3	4	5	6	7
EggWeight	0.23	0.81	0.79	0.66	0.38	0.25	0.37
Hatch	0.17	0.52	0.58	0.59	0.55	0.14	0.08

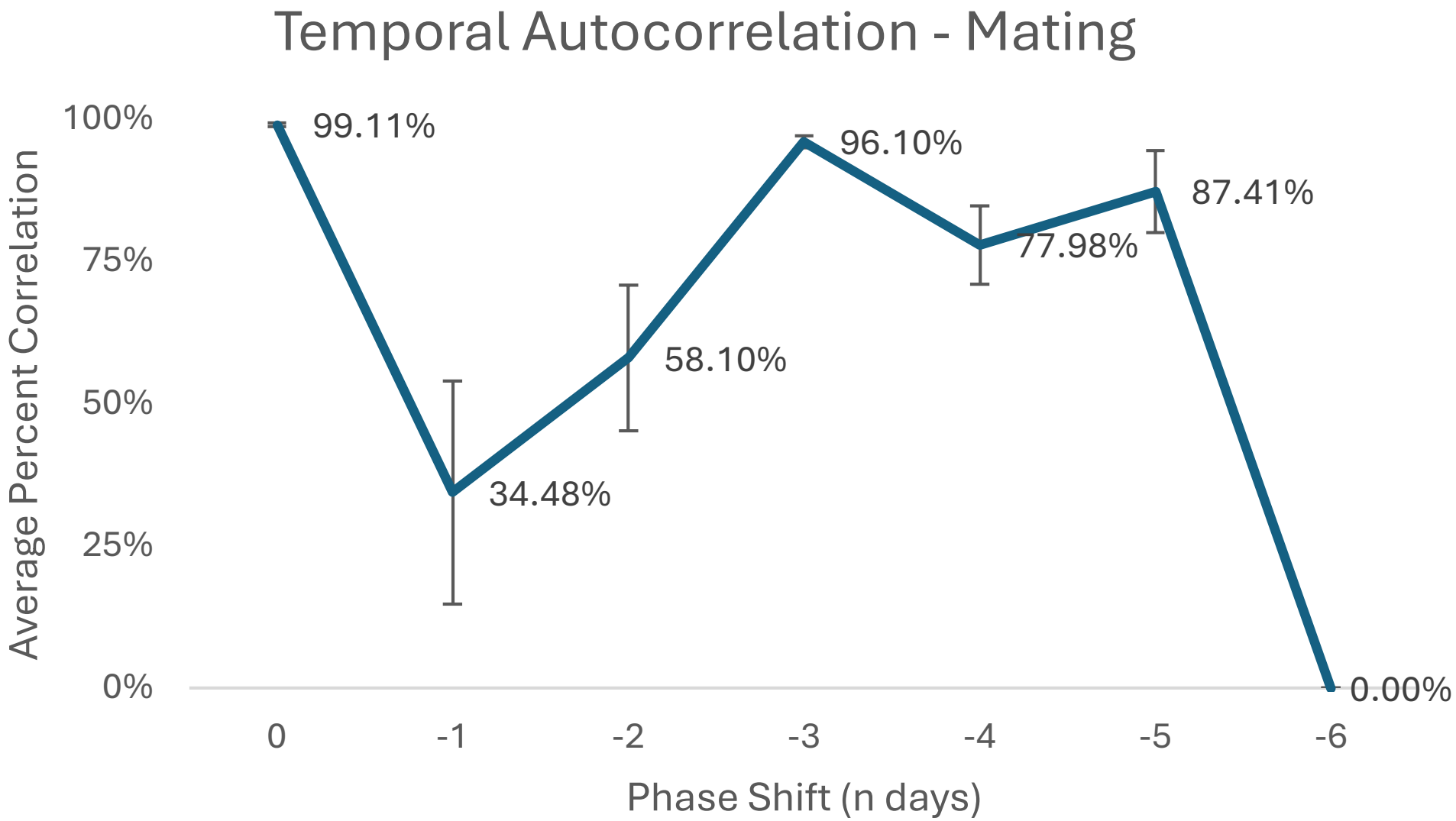
Temporal Autocorrelation - Mating
Average Percent Correlation
100%
75%
50%
25%
0%
99.11%
34.48%
58.10%
96.10%
77.98%
87.41%
0.00%
0
-1
-2
-3
-4
-5
-6
Phase Shift (n days)

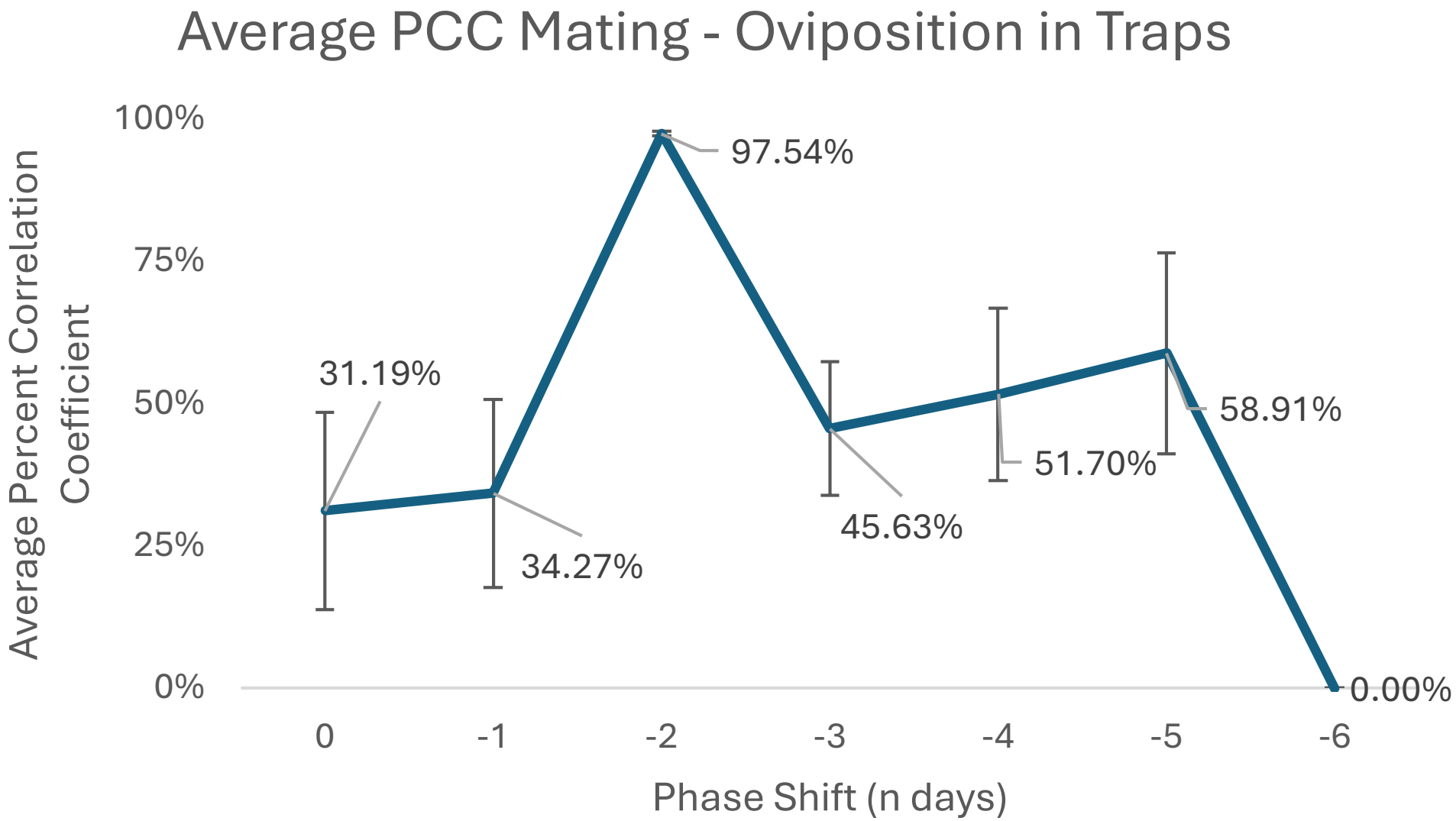
Average PCC Mating - Oviposition in Traps
Average Percent Correlation Coefficient
100%
75%
50%
25%
0%
97.54%
31.19%
58.91%
51.70%
45.63%
34.27%
0.00%
0
-1
-2
-3
-4
-5
-6
Phase Shift (n days)

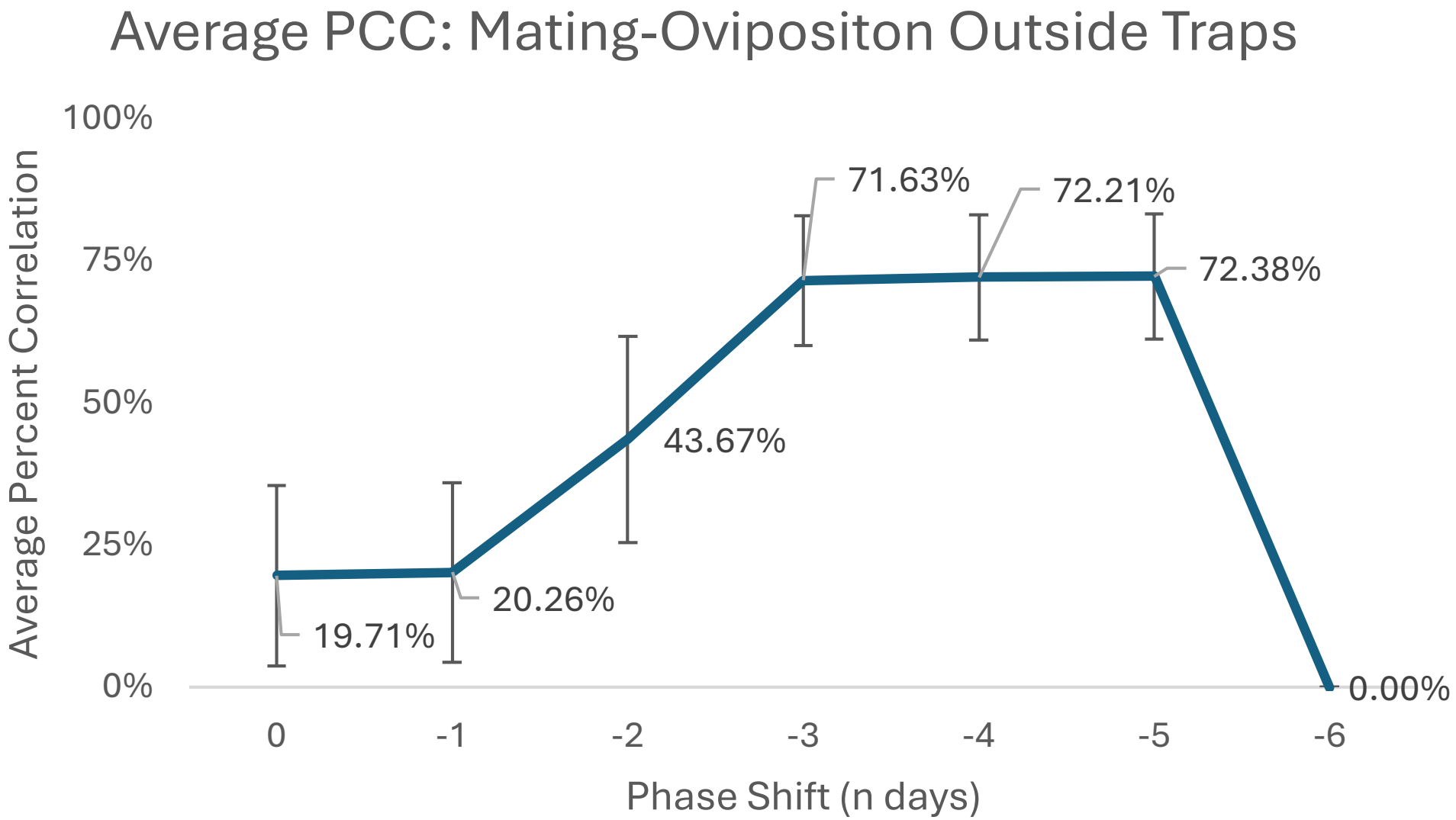
Average PCC: Mating-Ovipositon Outside Traps
Average Percent Correlation
100%
75%
50%
25%
0%
71.63%
72.21%
72.38%
43.67%
20.26%
19.71%
0.00%
0
-1
-2
-3
-4
-5
-6
Phase Shift (n days)

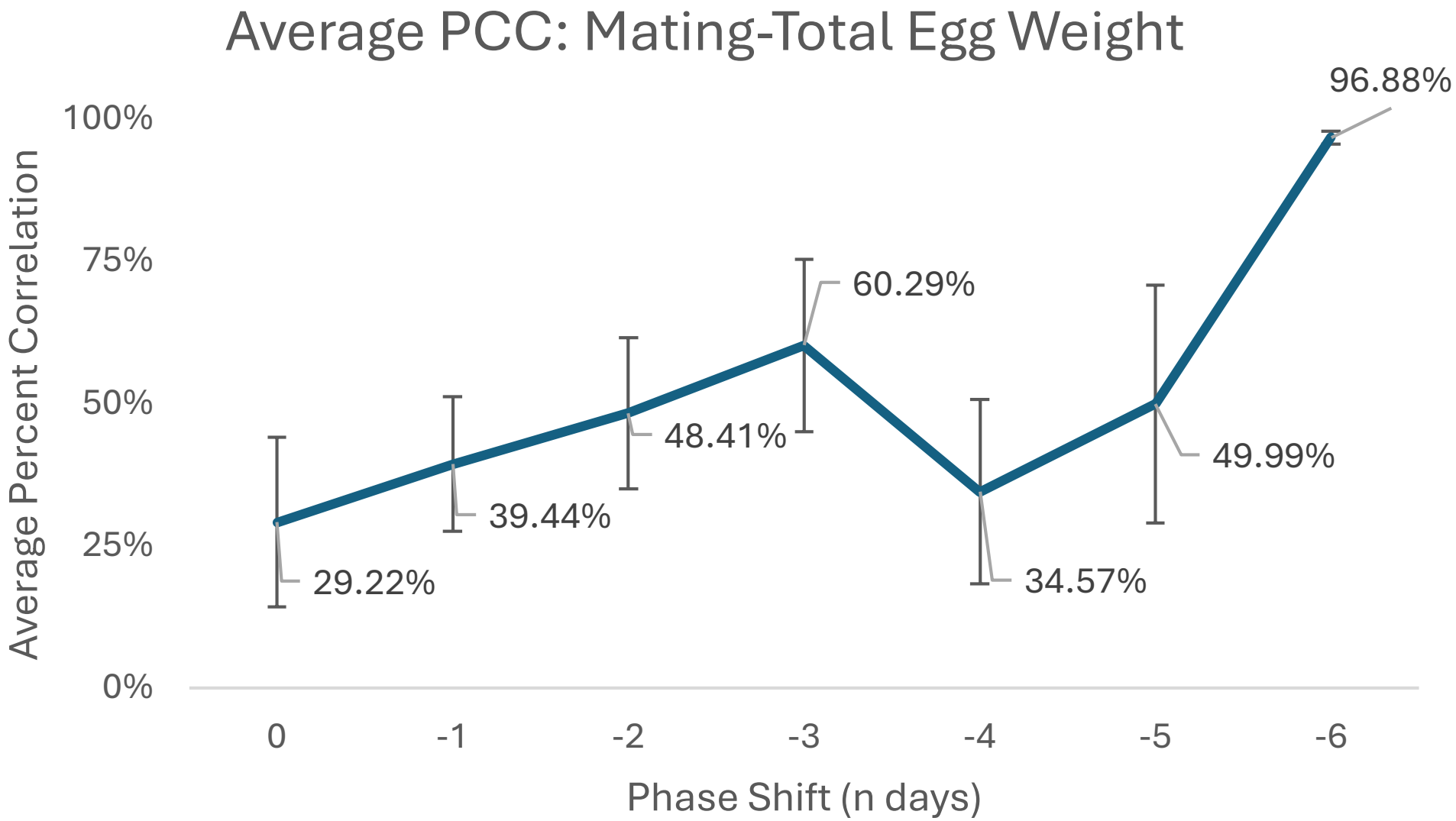
Average PCC: Mating-Total Egg Weight
Average Percent Correlation
100%
75%
50%
25%
0%
29.22%
39.44%
48.41%
60.29%
34.57%
49.99%
96.88%
0
-1
-2
-3
-4
-5
-6
Phase Shift (n days)

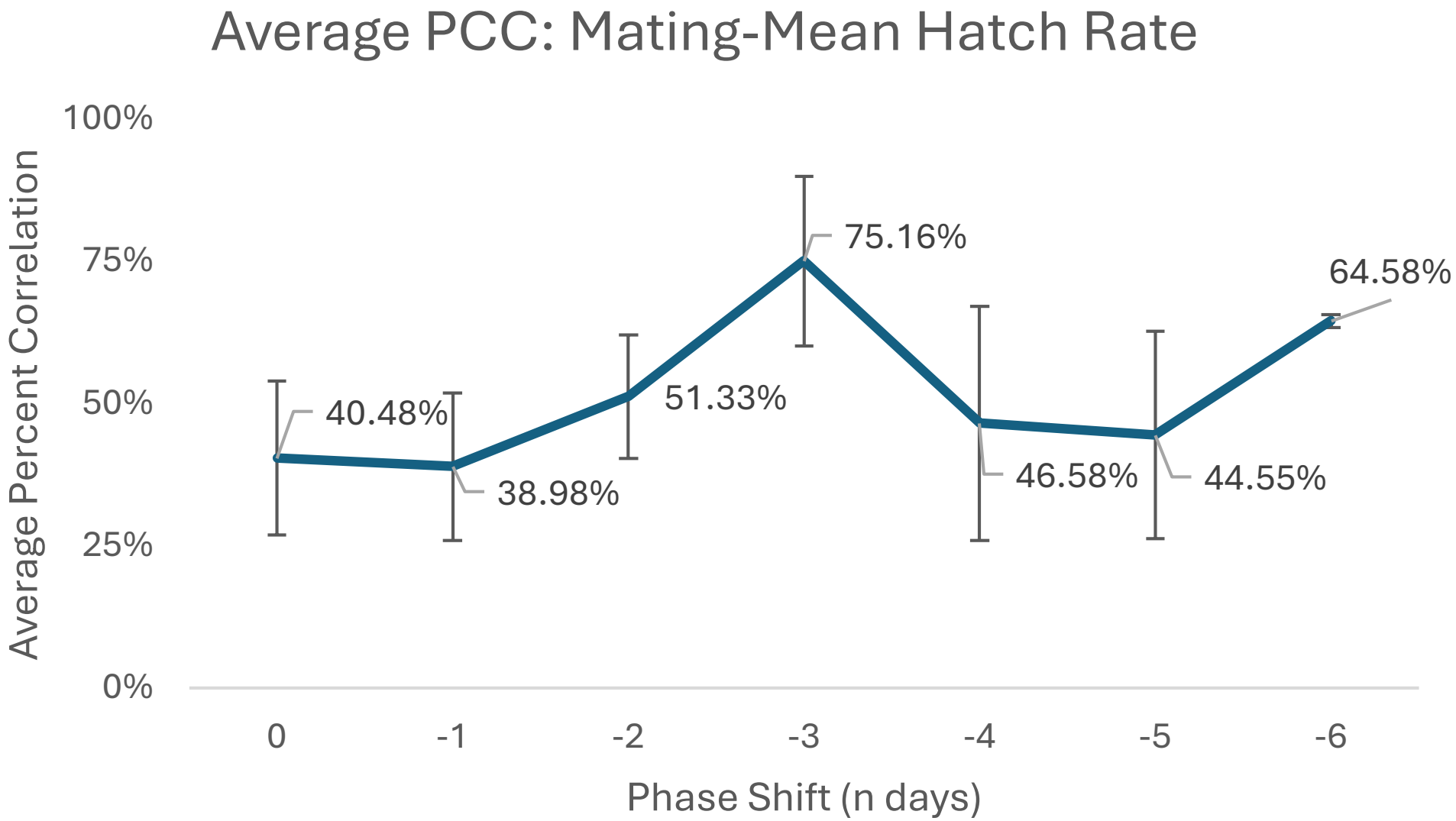
Average PCC: Mating-Mean Hatch Rate
100%
75%
50%
25%
0%
Average Percent Correlation
40.48%
38.98%
51.33%
75.16%
46.58%
44.55%
64.58%
0
-1
-2
-3
-4
-5
-6
Phase Shift (n days)

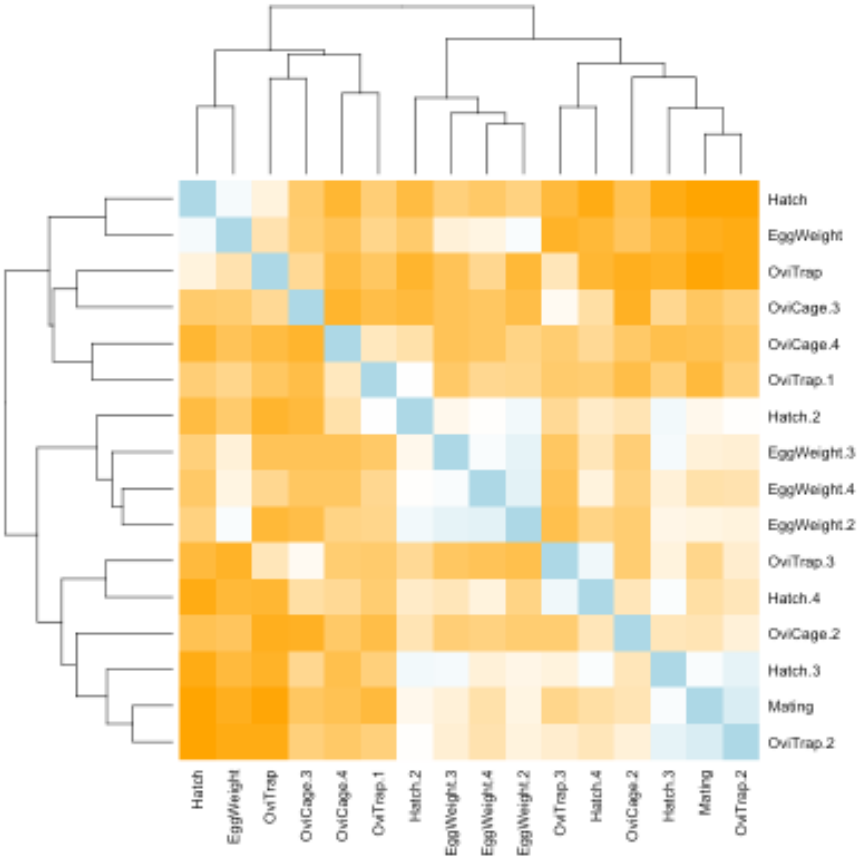
Hatch
EggWeight
OviTrap
OviCage.3
OviCage.4
OviTrap.1
Hatch.2
EggWeight.3
EggWeight.4
EggWeight.2
OviTrap.3
Hatch.4
OviCage.2
Hatch.3
Mating
OviTrap.2